https://doi.org/10.48047/AFJBS.6.16.2024.1318-1347

African Journal of Biological Sciences

Journal homepage: http://www.afjbs.com

Research Paper Open Access

Gamma-linolenic acid functionalized liposomes to improve anticancer efficacy of paclitaxel

Dharmendra Kumar[1#], Rohit Kumar[1], Anurag Kumar[1], Sneha Yadav[1], Jyoti Singh[1], Archana Bharti Sonkar[1], Neeraj Kumar Shrivastava[1], Pratibha Verma[1], Mohd Nazam Ansari [2], Abdulaziz S. Saeedan[2], Gaurav Kaithwas[1,*]

1.Department of Pharmaceutical Sciences, Babasaheb Bhimrao Ambedkar University (A Central University)

2. Department of Pharmacology and Toxicology, College of Pharmacy, Prince Sattam Bin Abdulaziz University, Al-Kharj, KSA

#First Author: Dharmendra Kumar
Email: vermadharmendra135@gmail.com

***Corresponding Author:**Dr. Gaurav Kaithwas
(Professor)Department of Pharmaceutical Sciences,
Babasaheb Bhimrao Ambedkar University (A Central University),
Vidya Vihar, Raebareli Road,
Lucknow-226 025, (U.P.), India
Phone: +91-522-2998129, +91-9670204349
Email: gauravpharm@hotmail.com, gauravpharm@gmail.com

Volume 6, Issue 16, Dec 2024

Received: 15 Oct 2024

Accepted: 25 Nov 2024

Published: 09 Dec 2024

doi: 10.48047/AFJBS.6.16.2024.1318-1347

Abstract

Paclitaxel (PTX), a cytotoxic drug, primarily acts on microtubules. At high concentrations, Cell cycle arrest is primarily caused during the G2/M phase. polyunsaturated fatty acid gamma-linolenic acid (GLA), shows cytotoxic effects on different cancer cell types. In combination, it synergistically enhanced anti-tumorigenic activity of chemotherapeutic agents. This investigation is focused on the formulation, optimization, and characterization of PTX-GLA liposomes and their efficacy in combating breast cancer. GLA primarily replaces lipid constituents within liposomes to enhance the anticancer efficacy of PTX-GLA liposome. It was prepared using the thin film hydration method and optimized through Box-Behnken design employing Design-Expert software. The PTX-GLA liposome was characterised on the basis of its size, shape, and surface characteristics using zeta potential analysis, scanning electron microscopy (SEM), and transmission electron microscopy (TEM). Fourier-transform infrared (FTIR) spectroscopy confirmed the compatibility of PTX-GLA-liposomes. The in-vitro drug release tests demonstrated that the PTX-GLA liposome exhibited sustained and regulated release kinetics over a duration of 48 hours, while maintaining excellent stability. The IC50 values of PTX liposomes, GLA liposomes, and PTX-GLA liposomes against MCF-7 cells were determined to be IC50 11.61 µM,12.31 µM and 11.21 µM, respectively. Cellular uptake investigations on MDA-MB-231 cells demonstrated enhanced internalization of PTX-GLA liposomes compared to GLA liposomes. Additionally, the anti-inflammatory properties of GLA may mitigate specific adverse effects associated with chemotherapy. The synergistic combination of GLA and Paclitaxel may enhance the overall efficacy of treatment through mechanisms such as anti-inflammatory and pro-apoptotic actions.

Graphical abstract

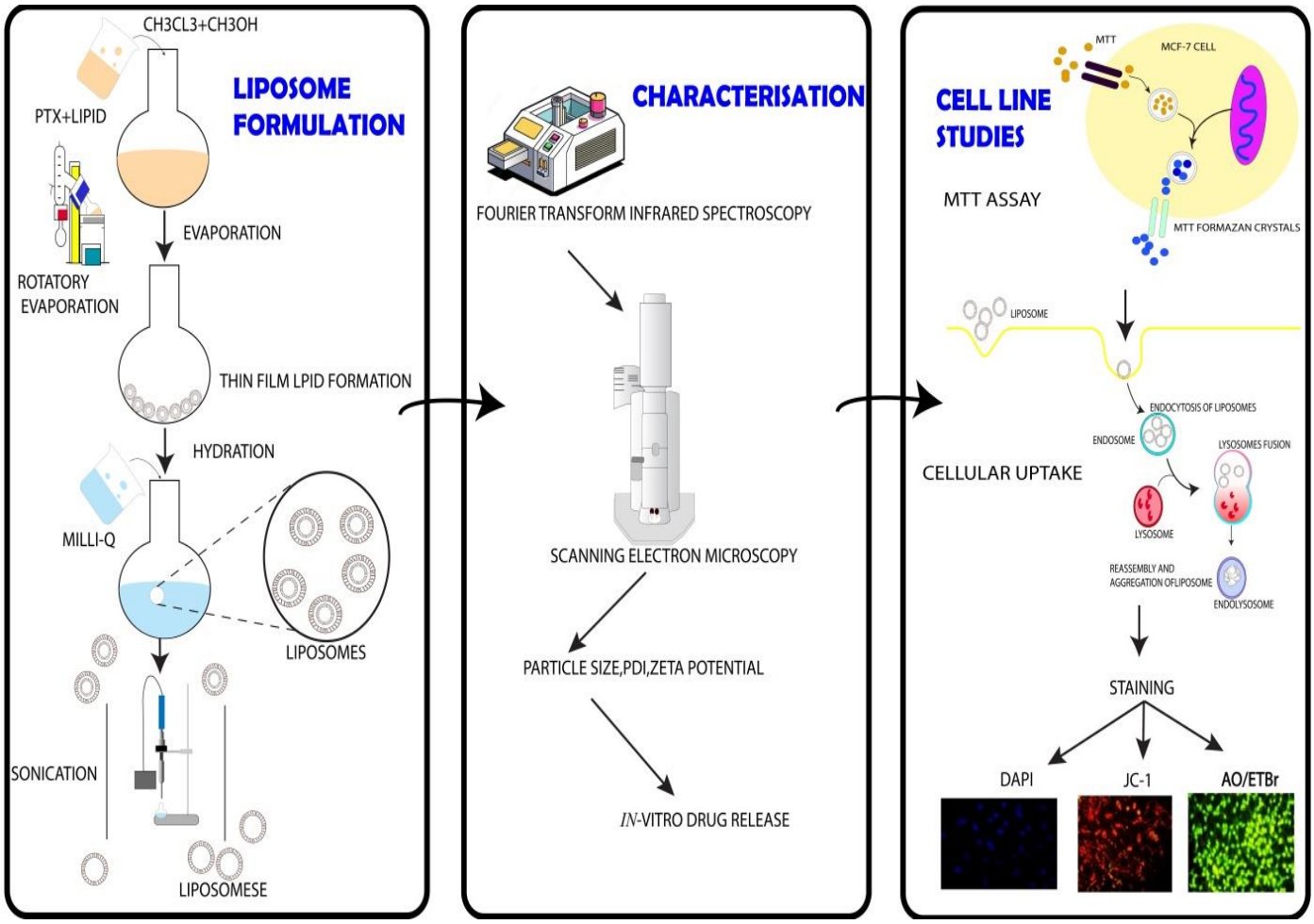

Keywords: Paclitaxel, Gamma- Linolenic acid, Liposomes, PTX-GLA Liposome, Breast cancer.

Abbreviation

GLA Gamma-linolenic acid

PTX Paclitaxel

PC Phosphatidylocholine

Chol Cholesterol

TPGS D-α Tocopherol polyethylene glycol

FTIR Fourier Transform Infrared Spectroscopy

SEM Scanning electron microscopy

TEM Transmission electron microscopy

P S Particle size

PDI Polydispersity index

ZP Zeta potential

PUFA Polyunsaturated fatty acid

MTT 3-(4, 5-Dimethylthiazol-2-yl)-2, 5-Diphenyltetrazolium Bromide

EE Entrapment efficiency

1. Introduction

Cancer is the crucial factor responsible for death global and a significant obstacle to improving average life[1,2]. Among women, breast cancer is the most predominant and the primary cause of cancer-related mortality. In 2022, the global incidence of breast cancer in women was estimated to be around 2.3 million, making up 11.6% of all newly diagnosed cancer cases. Furthermore, breast cancer was responsible for approximately 670,000 deaths, which represents 6.9% of all deaths due to cancer [3]. Paclitaxel (PTX), a class of microtubule-stabilizing drugs, is an effective chemotherapeutic agent, demonstrating significant efficacy in managing a diverse range of malignancies, including breast, ovarian, skin, and lung cancers. PTX stabilises microtubules, inhibiting cell division and inducing apoptosis in fast-growing cancer cells. Due to its high toxicity, lipophilicity, low water solubility, short half-life, and difficulties achieving tumour site drug concentration, PTX has a restricted treatment window [4,5]. To improve bioavailability, half-life, and toxicity, recent research have explored formulation modification, combination therapy, and targeted therapy [6]. A typical lipid-based formulation contains "liposomes," made of phospholipids. Due to their well-organized structure, liposomes may load and disperse substances of different solubility. The water/lipid bilayer interface has amphiphilic molecules, the lipid bilayer has hydrophobic molecules, and the aqueous core has hydrophilic molecules [7,8] . It has been found that lipid-based nanocarriers showed an advantage over other formulation strategies to increase drug bioavailability [9]. Liposomes protect medications against physiological circumstances such as enzymatic degradation, chemical and immunologic inactivation, and fast elimination from the bloodstream. This protection of liposomes enhances and prolongs their therapeutic effects. Hydrophobic drugs, such as PTX encapsulation, can potentially improve PTX's solubility, bioavailability, and therapeutic index. Functionalizing liposomes with bioactive lipids has emerged as a promising strategy to improve their therapeutic potential further [10,11]. Gamma-linolenic acid (GLA) is classified as an omega-6 polyunsaturated fatty acid (PUFA). It is also known by its chemical name, cis-6, 9, and 12-octadecatrienoic acid. Omega-6 fatty acids also treat inflammation, arthritis, and cancer. Reports also suggest that it aids in weight control, enhances immunity, and regulates mood. Research studies have shown the

ability of GLA to fight cancer by promoting the formation of free radicals, lipid peroxidation, and macrophage activation [12,13]. Since the human body cannot produce it independently, we classify it as an essential fatty acid, typically obtained through diet or supplementation Evening primrose, borage, and black currant seed oil are among the plant oils containing GLA [14]. GLA can induce programmed cell death, halt cancer cell proliferation, and modulate the immune response. These characteristics make it an appealing natural agent for cancer treatment. Combining GLA with other drugs can enhance its efficacy and reduce its toxicity. Adding GLA to liposomal formulations might have two benefits: it might make PTX more effective against cancer while also lowering the harmful effects that come with it. GLA and Paclitaxel may work better to treat cancer cells when encapsulated in liposomes. This study aims to investigate the anticancer properties of the GLA-PTX liposome. We will investigate the mechanisms through which GLA improves the effectiveness of PTX, the process of making and analysing GLA-functionalized liposomes, and the assessment of their anticancer activity and toxicity profile in laboratory and animal studies. This technique enhances the outcomes of cancer patients by offering a chemotherapy option that is both safer and more effective [10,15] .

2. Material and methods

2.1 Materials

GLA was bought from TCI chemicals (India) Pvt. Ltd. PTX, which was a kind gift sample from by Fresenius Kabi Oncology Limited in Gurugram, India. Phosphatidylocholine, Cholesterol was procured from MP Biomedicals, LLC. 29525 Fountain Parkway. Solon, Ohio 44139. D-alpha-tocopheryl polyethylene glycol 1000 succinate (TPGS) were procured from Sigma Aldrich. The MCF-7 cell lines were procured from NCCS, Pune, India. Dulbecco Phosphate Buffered Saline (DPBS) (Gibco, 14200075, USA), Antibiotic-antimycotic (100X) and Trypsin (Gibco, 25200072, USA) were purchased from Gibco, USA. 4', 6-diamidino-2-phenylindole (DAPI) was acquired from purchased from Sigma Aldrich, Saint Louis, MO, USA. Acridine orange Ethidium bromide (AO/ EB) and MTT were procured from Himedia Laboratories Pvt.Ltd.Vadhani Mumbai India. The JC-1 assay kit (Thermo Scientific, M34152), DMSO were procured from (D1435, Sigma Aldrich, Saint Louis, MO, USA. The experiment was conducted using Milli–Q Evoqua Water Technologies Gunzburg

Auf der Weide 10 89312 Gunzburg Germany. Dialysis membrane, with a molecular weight cut off ranging from 12,500 to 14,000 daltons, was Himedia Laboratories Pvt.Ltd.Vadhani Mumbai India. The ACN and water used were of HPLC grade, found from Merck Darmstadt, Germany. All the remaining chemicals and reagents used were of high quality.

2.2 Preparation of liposomes

PTX-GLA-loaded liposomes were developed by slight modifications to the thin-film hydration method. 10ml of a 1:1 (v/v) chloroform: methanol combination were used to dissolve phosphatidylcholine, cholesterol, TPGS, PTX, and GLA in a round-bottom flask. To create a thin film, the organic solvents were thereafter gradually evaporated in a rotating evaporator while under vacuum. To eliminate any remaining organic solvents, the film was further dried for 4 hours at 25°C in a vacuum oven. The thin film was then rotated at 100 rpm for 2 hours while it was hydrated with milli-Q water. to produce vesicles of a constant size, the liposomal dispersion finally used the LABMAN-PRO-650 device to perform probe-sonication for the proper amount of time. These vesicles were then dried by freezing[16–18] .

2.3 Optimization of Liposomes formulation by using (DoE) Software

A Box-Behnken Response Surface design optimized three process parameters at three levels. Based on existing information and accessible literature, GLA/PC ratio and total lipid content were chosen as optimization parameters, while PS, PDI, and Zeta potential were considered responses. (Design Expert Version -13) Stat-Ease® version 13.0.5.0 was used to construct 17 experimental runs. All the results of the experiments were adjusted to a quadratic polynomial model. The model selection process involved assessing several statistical metrics, such as R^2, Sequential Model Sum of Squares, Lack of Fit, and the partial sum of squares from analysis of variance (ANOVA). After careful evaluation, the most appropriate model was selected [16,19] .

3. Characterization

3.1 Particle Size, PDI and ZP

The improved liposomal formulations were analysed for particle size (PS), polydispersity index (PDI), and zeta potential (ZP) using a Litesizer 500 device produced by Anton Paar Instruments [16].

3.2 Fourier Transform Infrared Spectroscopy (FTIR) analysis

The FTIR exploration (Thermo Scientific, USA Nicolet 6700) was used to investigate potential intermolecular interactions between the components of PTX-GLA-loaded liposomes. The FTIR spectra of pure PTX, pure GLA, blank liposomes (without drugs), and PTX-GLA-loaded liposomes were compared. The FTIR spectrophotometer was used to record the spectra in the range of 4000 cm-1 to 400 cm-1 [20].

3.3 Scanning electron microscopy (SEM)

The samples' surface texture was analysed using scanning electron microscopy (SEM). according to the previously outlined methods. Briefly, one drop of formulation was carefully poured on aluminium foil, and each specimen underwent dehydration via critical point drying before SEM examination (JEOL JSM-6490LV, Japan)[21].

3.4 Transmission electron microscopy (TEM)

The developed formulation was analyzed for shape and surface morphology using the TEM (Model: Jeol JEM 1400, Jeol Ltd., Tokyo, Japan). In conclusion, ultrapure water was used to dilute the samples. Next, a little amount of the liposome formulations that had been diluted was applied to a copper grid that had been covered with Formvar. After dryingThe sample was coated with a 1% (w/v) phosphotungstic acid solution to develop a stain. Finally, a transmission electron microscope (TEM) was employed to examine the material, with an accelerating voltage of 80 Kv [22].

3.5 Entrapment efficiency

To quantify entrapped PTX, The liposomal dispersion performed centrifuged at a speed of 10,000 rpm was for a duration of 10 minutes in order to separate and collect the PTX that was not compressed inside the liposomes. The supernatant, which contained liposomes loaded with PTX, was subjected to ultra-centrifugation at 15,000 rpm for 30 minutes at 4°C in order to remove the unbound drug. The PTX-liposome pellet was dissolved in acetonitrile, and its concentration was quantified using a validated ultraviolet (UV) method [16,19].

$$EE = \frac{\textbf{Total amount of PTX – Amount of PTX in the supernatent}}{\textbf{Total amountof PTX}}$$

3.6 *In-vitro* drug release studies

PTX-GLA-loaded liposomes' *in-vitro* release of PTX was evaluated by means of a dialysis bag distribution method. In summary, a 1000 Da molecular weight cut-off cellulose membrane dialysis bag was filled with 10 mg of PTX-GLA liposomes (in 10 ml). Next, a volume of 50 ml of phosphate-buffered saline (PBS) with a pH of 7.4 was introduced into the sealed bag and subjected to continuous agitation at a speed of 100 rpm at a temperature of 37°C. At specified intervals, samples were taken out of the PBS and replaced with fresh medium. To measure the released PTX, the obtained samples were filtered and subjected to UV spectrophotometry analysis [16,23].

3.7 Stability studies

Accelerated stability study

PTX-GLA-loaded liposomes were tested for accelerated stability over 3 months as per the protocol described in our earlier report. Briefly, PTX-Lipo and PTX-GLA Lipo were kept in a stability chamber with temperatures stored at 4 ± 1°C and 40 ±2°C after 3 months; particle size, PDI, Z.P., and ease of reconstitution were all measured for the PTX-Lipo and PTX-GLA Lipo formulations [24].

3.8 *In-vitro* cell culture studies

The MCF-7 cells were acquired from the National Centre for Cell Science (NCCS) in Pune, India (Batch No.309/2023 Passage No.31). Subsequently, MCF-7 cells were cultured in DMEM media enriched with 10% FBS and a solution containing 100µg/ml of streptomycin and gentamycin. The cells were placed in a CO2 incubator that was kept at a temperature of 37 °C and had a CO2 concentration of 5%. The incubator was also kept humidified [25,26].

3.8.1 Cytotoxicity study

The MTT assay was employed to evaluate cell viability of the generated liposomes. Briely, MCF-7 cells (1x104) were evenly distributed into 96-well plates, with each well containing cells in triplicate. The cells were subjected to different concentrations (1 µM, 2.5 µM, 5 µM, 7.5 µM, 10 µM, 15 µM, and 20 µM) of GLA-Lipo, PTX-Lipo and PTX-GLA Lipo for a duration of 24 hours. After the incubation period, the liquid in each well was withdrawn and replaced with a new liquid containing 20 µl of MTT (5 mg/ml) solution for a duration of 4 hours. Subsequently, the medium was extracted from each well, and 100 µl of DMSO was used to facilitate the dissolution of the formazan blue crystals. Cell viability and IC50 (the concentration at which the

number of viable cells is reduced by 50%) were assessed using a microplate reader (SpectraMax ABS Plus, Rochester, NY, USA) by measuring the absorbance at 570 nm [27].

3.8.2 Cell uptake assay

An investigation was performed to examine the uptake of liposomes by cells using coumarin-6 (C-6) as a model dye. A 12-well plate with a coverslip was seeded with 5×10^5 MDA-MB-231 cell lines per well, and it was then incubated for 24 hours at 37 ºC with 5% CO2 in the air. The many liposome formulations loaded with C-6 dye were treated for 4 hours after the cells attained 70% confluence. The media was withdrawn and the cells were rinsed 3 times with PBS (7.4) following a 4 hours incubation period with various dye-loaded formulations. Following washing, the cells were fixed for 30 minutes using 4% paraformaldehyde (PFA). Next, for 10 minutes, the cells were permeabilized using a 0.1% triton-x-100 solution. 1 ml of DAPI solution (2.5 µg/ml) was used after permeabilization, and it was incubated in a dark environment for 10 minutes. After incubating with DAPI, the cells were washed with cold PBS (pH 7.4). Following the removal of the coverslip, a fixative solution was applied to the glass slide to firmly attach it. The cellular uptake pictures were acquired using an inverted laser scanning confocal microscope (ILCSM, LSM-900, and Zeiss, Germany) [25].

3.8.3 Nuclear morphology detection using DAPI

MCF-7 cells at a confluence of 70% were placed onto a 6-well plate and subjected to ½ IC50 and IC50 concentrations of Placebo-Lipo ,PTX-Lipo, GLA-Lipo, and PTX-GLA Lipo for a duration of 24 hours. After the incubation period, PBS was used to rinse the treated and untreated cells, and then 4% paraformaldehyde in PBS was added to fix them for 10 minutes. Following fixation, the cells were treated with DAPI (5 µg/mL) for a duration of 20 minutes. An inverted fluorescent microscope (IX53, Olympus Japan) with a 20X magnification was used to examine nuclear alterations [19].

3.8.4 Detection of Apoptosis using A.O./EtBr staining

A.O./EtBr staining was utilized in inverted fluorescence microscopy to determine apoptotic morphological changes. Briefly, In a 6-well plate, MCF-7 cells were seeded and then incubated. with ½ I.C. 50 and IC50 of PTX-Lipo, GLA-Lipo and PTX –GLA Lipo for 24 hrs. After picking, treated and untreated control cells were cleaned with

PBS and stained with A.O. (100µg/ml) and EtBr (100µg/ml) staining solution at 1:1 ratio for 5 min. Subsequently, Following a PBS wash, the cells were seen using an inverted fluorescent microscope. (IX53, Japan's Olympus) [27]**.**

3.8.5 Mitochondrial membrane potential using JC-1 dye

Alterations in the mitochondrial membrane potential (ΔΨm) which may be seen using JC-1 dye, were suggestive of apoptosis. To summarise, MCF-7 cells were placed on 6-well culture plates and treated with GLA-Lipo, PTX-Lipo and PTX-GLA Lipo at doses equivalent to half of the IC50 and the IC50 for 24 hours. After the treatment, the cells underwent three washes with PBS and were thereafter exposed to 100 µL of JC-1 dye solution for 30 minutes. After the procedure of staining, the cells were washed with PBS and examined using FITC and TRITC filter sets on an inverted fluorescent microscope. microscope (IX 53, Olympus, Shinjuku, Tokyo, Japan). [26,27].

3.9 Statistical Analysis

All data is shown as mean values complemented by the associated standard deviations (S.D.). The numerical study was accomplished using Graph Pad Prism Version 8.0.1 (Graph Pad Software) and included doing a one-way ANOVA, followed by Dunnett's multiple comparisons test. The MCF-7 cell line performed staining experiments using DAPI, JC-1, and A.O./EtBr dyes. The study was performed using the Image J1.53e software developed by the (National Institute of Health) in the United States.

4. Results

4.1 Optimization of Liposomes formulation by using (DoE) Software

The Box-Behnken design optimised the formulation by seeing 3 separate factors at 3 levels. 17 runs were recommended, as shown in **Table 1**. Box-Behnken experimental design illustrates the 3-D surface plots of particle size (A to C), PDI (D), and Z.P. (E and G), and the 3-D surface plot in **figure 1**.

Figure 1

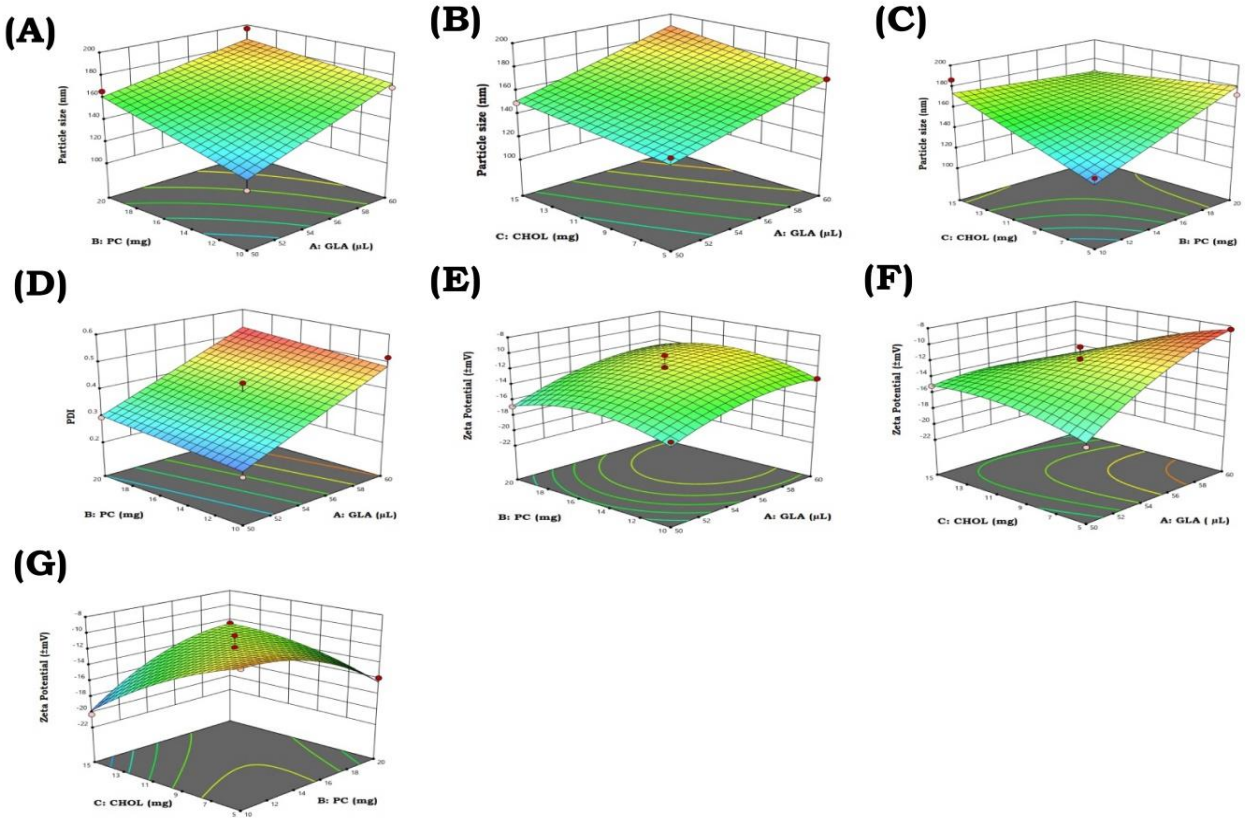

Figure 1

Box-Behnken experimental design illustrating the 3-D surface plots of (A to C), represents the effect on P.S., (D) represents the effect on PDI and (E to G) represents the effect on Z.P.

Table 1:

Box-Behnken experimental design illustrating the results of different variables and Responses measured during a 17-run period. GLA and pPhosphatidylocholine cholesterol ratio were chosen as optimization parameters, while PS, PDI, and ZP were considered responses.

Std	Run	Factor 1 A:GLA µL	Factor 2 B:PC mg	Factor 3 C:CHOL mg	Response 1 Particle size nm	Response 2 PDI	Response 3 Zeta Potential ±mV
17	1	55	15	10	160.26	0.424	-10.4
12	2	55	20	15	165.85	0.459	-12.5
2	3	60	10	10	169.21	0.517	-13.5
7	4	50	15	15	149.62	0.239	-15.1
11	5	55	10	15	186.43	0.361	-20.3
4	6	60	20	10	196.43	0.498	-13.2
1	7	50	10	10	118.21	0.236	-16.3
10	8	55	20	5	172.21	0.364	-15.9
6	9	60	15	5	169.99	0.508	-8.4
5	10	50	15	5	142.07	0.305	-17.6
16	11	55	15	10	160.26	0.424	-11.9
15	12	55	15	10	160.26	0.424	-11.9
14	13	55	15	10	160.26	0.424	-11.9
8	14	60	15	15	182.42	0.463	-15.8
13	15	55	15	10	160.26	0.424	-13.9
9	16	55	10	5	131.92	0.318	-10.2
3	17	50	20	10	165.86	0.294	-16.8

4.2 Particle Size, PDI and ZP

The formulations PS, PDI, and ZP were assessed and tabulated in Table 1. Based on PS, PDI, ZP and maximum GLA content in the liposome, the optimized formulation was chosen and taken for further analysis **(Table 2).**

Table 2

PS distribution, ZP, PDI and Entrapment efficiency of PTX-Lipo and PTX-GLA Lipo Values are presented as mean ±SD (n=3).

Sample	**Particle size (nm)**	**Polydispersity index (PDI)**	**Zeta potential (mv)**	**%EE**	
				PTX Lipo	**PTX-GLA Lipo**
Placebo-Liposome	104.21 ±1.31	0.262±0.011	-10.3±0.72	80.28%	77.92%
PTX-Liposome	161.2 ±4.01	0.238±0.002	-17.6±2.05		
GLA-Liposome	150.99 ±2.12	0.263±0.003	-14.9±0.91		
PTX-GLA-Liposome	186.43 ±1.03	0.361±0.015	-20.3±0.8		

4.3 Fourier Transform Infra-Red Spectrometer (FTIR)

FT-IR analysis of all the excipients, drugs and formulations is depicted in **Figure 2**. The PTX represented the prominent characteristic peaks around 1713.3 and 1240.6 cm^{-1}. 1713.3 cm^{-1} represents stretching vibrations of the carbonyl group (C=O) present in the PTX taxane ring structure. Further, 1240.6 cm^{-1} represents the stretching vibrations of the ester functional group (C-O-C), confirming the taxane ring structure of PTX. The 2927.5 cm-1 broad peak signifies the C-H stretching vibrations, confirming the unsaturated fatty acid chain in GLA. Moreover, a sharp peak around 1710.3 cm^{-1} shows stretching vibrations of the carbonyl group (C=O) in GLA's carboxylic acid functionality. The characteristic peak at 2939.6 and 1461.5 cm^{-1} in TPGS reveals aromatic C-H stretching vibrations and stretching vibrations of the phenyl rings present in TPGS. The peaks in PTX-GLA-LIPO (1639.5 and 3475.4 cm-1) represent the successful incorporation of PTX and GLA in liposome structure**.**

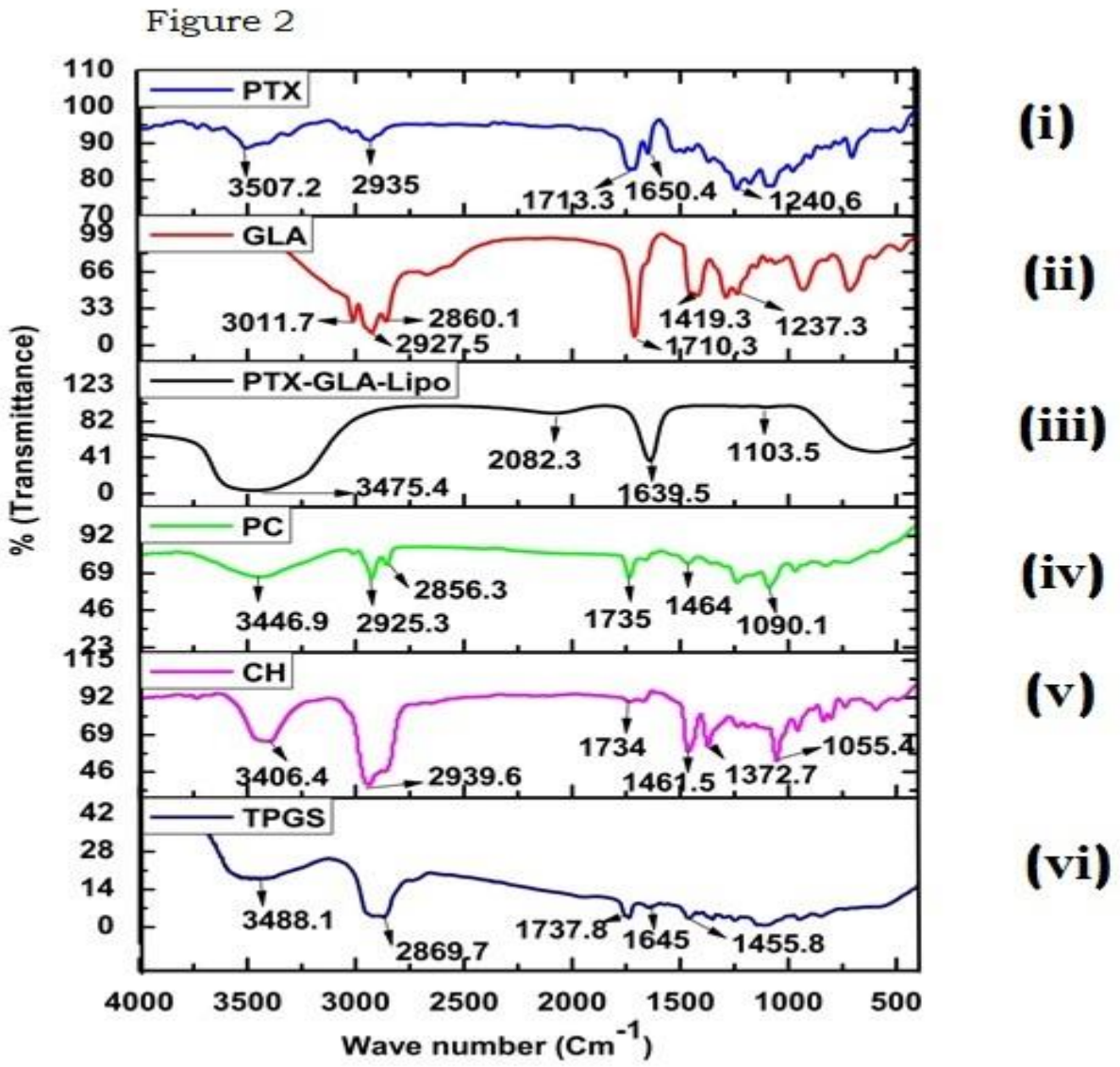

Figure 2

The FTIR spectra of (i) PTX (ii) GLA (iii) PTX-GLA liposomes (vi) P.C. (v) C.H. (vi) TPGS compared to the spectra of pure PTX, GLA, and PTX-GLA Lipo indicate the different wave numbers of the functional group.

4.4 Surface morphology

The optimized liposome was analyzed for shape and surface morphology by SEM and TEM analysis, and we observed the spherical and unilamellar particles. SEM and TEM analysis investigated the morphology of liposomal formulations. As depicted in **Figures (A)** Placebo-Lipo (B) PTX-Lipo (C) GLA-Lipo (D) PTX-GLA Lipo and TEM

analysis investigated figure (E) PTX-GLA-Lipo, all formulations of liposomes showed distinct spherical shapes.

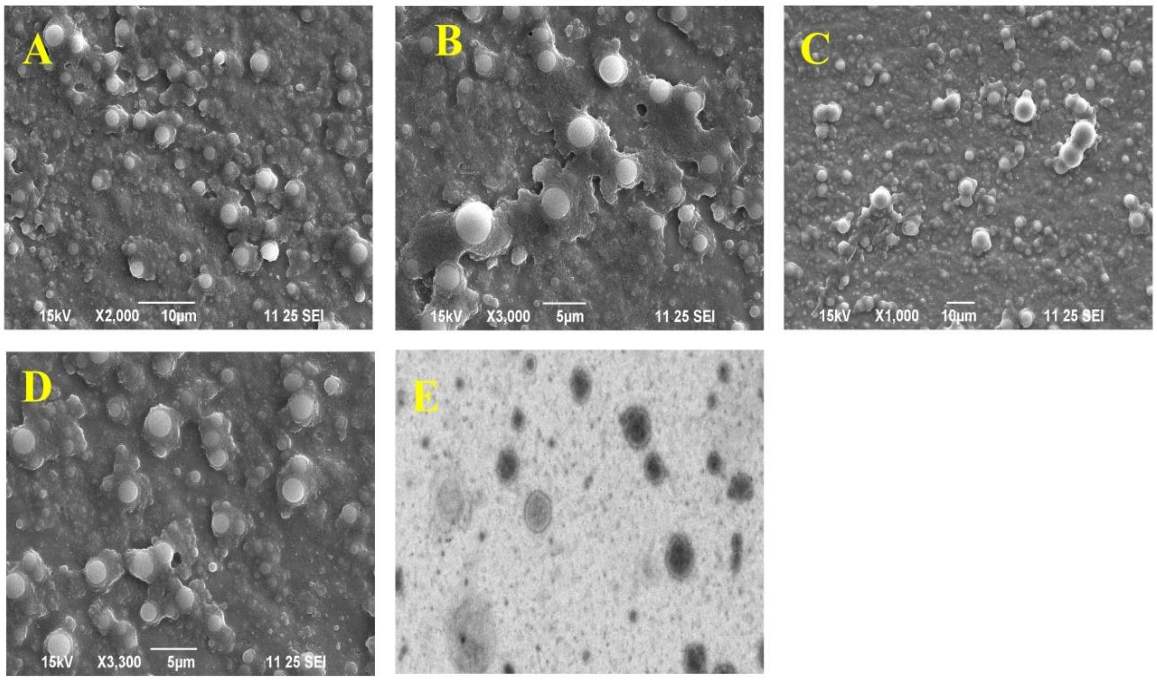

Figure 3

SEM and TEM analysis investigated the morphology of liposomal formulations. As depicted in Figures 3 (A) Placebo-Lipo (B) PTX-Lipo (C) GLA-Lipo (D) PTX-GLA Lipo and (E) PTX-GLA-Lipo, all formulations of liposomes showed distinct spherical shapes.

4.5 Entrapment efficiency

The entrapment of optimized liposomes was analyzed, and we observed 80.28% and 77.92% of PTX-Lipo and PTX-GLA Lipo, respectively **Table 2.**

4.6 *In-vitro* drug release

The percentage of PTX released from the PTX-Lipo and PTX-GLA Lipo in PBS buffer (pH 7.4) was determined at exact time intervals (0.5, 1, 2, 4, 8, 16, 24, 32 and 48 hours) and denoted in **figure 4**. The extended-release of PTX from formulation indicates a more controlled release behaviour.

Figure 4

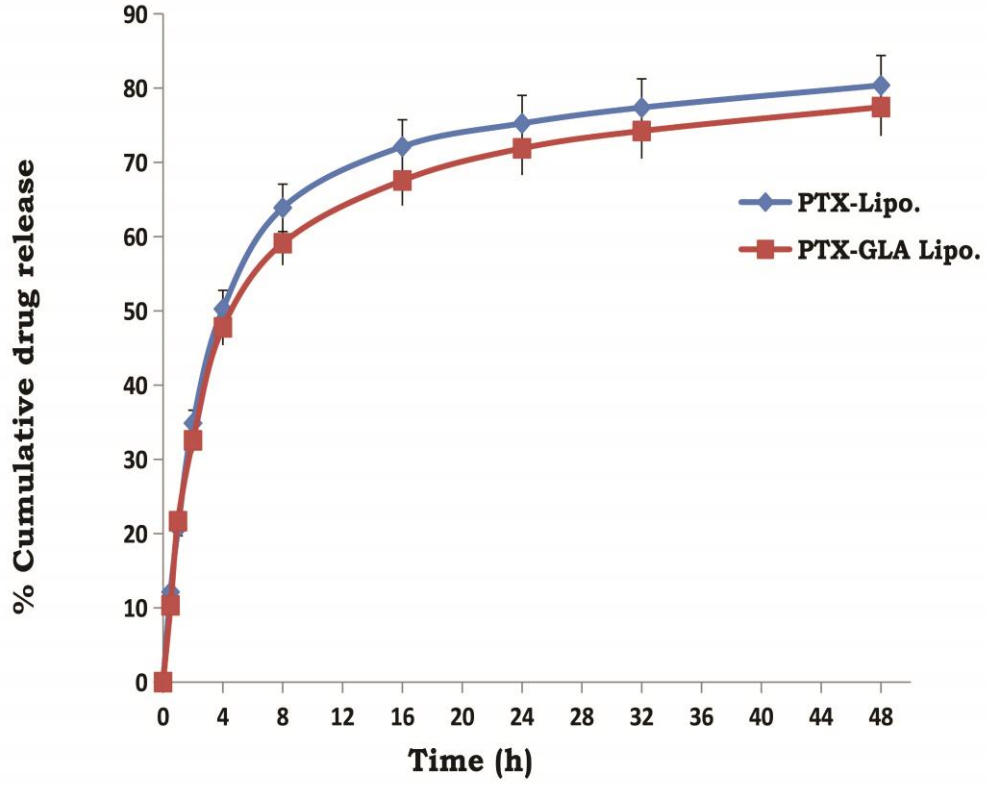

Figure 4 *In vitro* release curves of PTX-Lipo and PTX-GLA Lipo in PBS (pH 7.4) at 37°C The experiment was conducted in triplicate (n = 3).

4.7 Accelerated stability study

After its preparation and characterization, thePTX-Lipo and PTX-GLA-Lipo was promptly stored at 4 ± 1°C and 40 ±2°C. Measurements were recorded at both temperatures, like particle sizes, PDI and Zeta potential. **Table 3;** a slightly increase in the P.S., PDI, and Z.P. was reported after 3 months.

Table 3

Stability Initial and after 3 months of storage at two different temperatures 4 ± 1°C and 40 ±2°C, analyze PS, PDI, and ZP.

Liposome	**Initial**			**After 3 months**					
	PS (nm)	**PDI (%)**	**ZP (mV)**	4 ± 1°C			40 ±2°C		
				PS (nm)	**PDI (%)**	**ZP (mV)**	**PS (nm)**	**PDI (%)**	**ZP (mV)**
PTX- Lipo	161.2 ±4.01	0.238±0.002	-17.6± 2.05	185± 3.25	0.441 ±0.005	-1.42 ±0.017	238.4 ±6.023	0.442± 0.012	-22.9± 1.41
PTX-GLA Lipo	186.43 ±1.03	0.361±0.015	-20.3± 0.8	297.2 ±19.63	0.366 ±0.011	-15.1 ±1.47	337 ±8.54	0.473 ±0.006	-17.1 ±1.68

4.8 In-vitro studies

4.8.1 Cytotoxicity study with MTT

The cytotoxicity findings indicated that increasing the concentration of GLA-Lipo, PTX-Lipo and PTX-GLA liposomes to 1µM , 2.5 µM, 5 µM, 7.5 µM, 10 µM, 15 µM, and 20 µM inhibited MCF-7 cellular proliferation in a dose-dependent manner. The IC 50 values for GLA-Lipo, PTX-Lipo and PTX-GLA Lipo were 12.31µM.11.61 µM and 11.21 µM, respectively. The lowest I.C. 50 value was 11.21 µM for PTX-GLA Lipo **(Figure 5).**

Figure 5

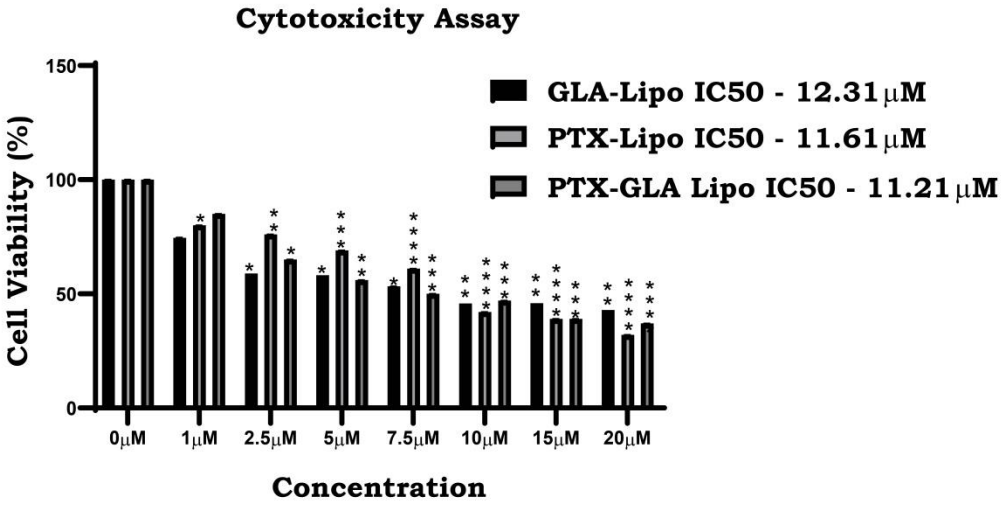

Figure 5

The graph revealed the ratio of living cells after a 24-hour incubation period with different concentrations of GLA-Lipo, PTX-Lipo and PTX-GLA-Lipo at a wavelength of 570nm. The data was reported as the mean value ±SD (n=3). We conduct the comparisons using a one-way ANOVA, followed by Dunnett's multiple comparisons test.

4.8.2 Cell uptake assay

The cellular internalization of all the formulations (GLA-Lipo, and PTX-GLA-Lipo) on MDA-MB-231 cells were investigated using confocal laser scanning microscopy (CLSM) **(Figure 6**). It was observed that the cellular uptake of PTX-GLA Lipo was significantly higher than that of other groups.

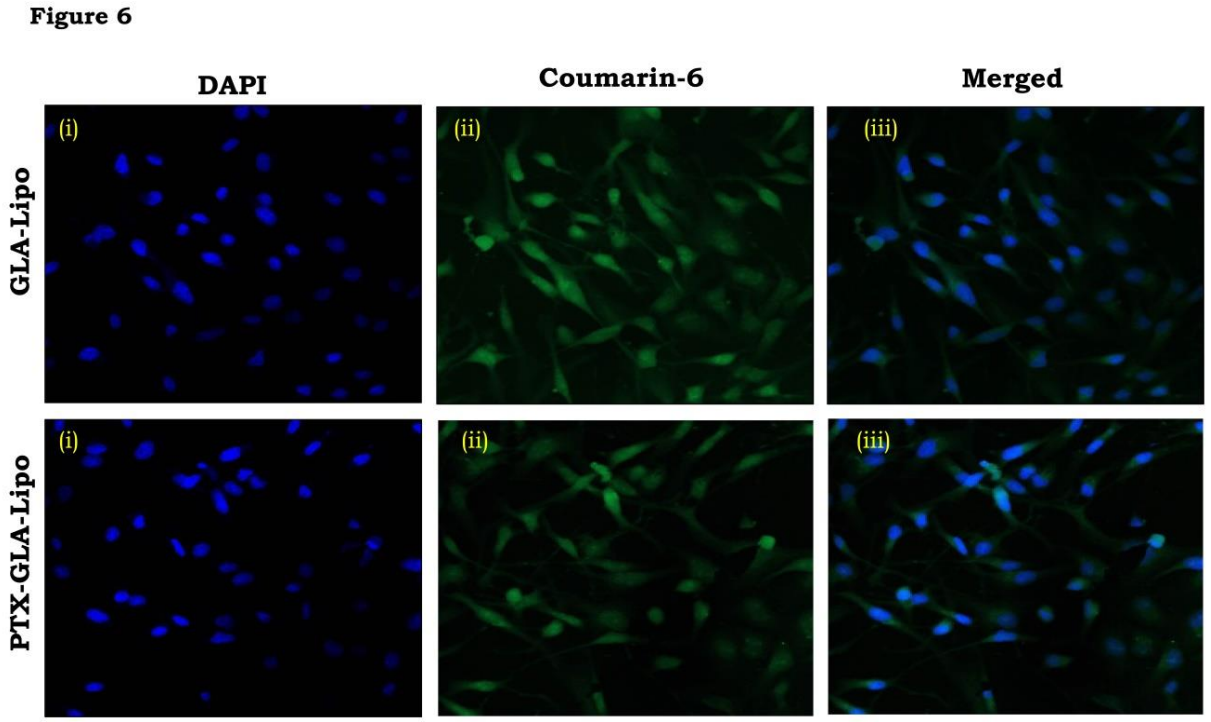

Figure 6

Cellular uptake of different liposomal formulations (GLA-Lipo and PTX-GLA Lipo) in MDA-MB-231 cell lines by confocal microscopy (**i)**, DAPI **(ii)**, Coumarin-6 and **(iii)** merged.

4.8.3 DAPI staining for detection of nuclear morphology

To assess chromatin condensation and nuclear fragmentation under an inverted fluorescence microscope, it was revealed that Placebo-Lipo, PTX-Lipo, GLA-Lipo, and PTX-GLA-Lipo showed vivid blue fluorescence, indicating nuclear apoptotic changes. However, untreated control MCF-7 cells showed clear round nuclei **(Figure 7).**

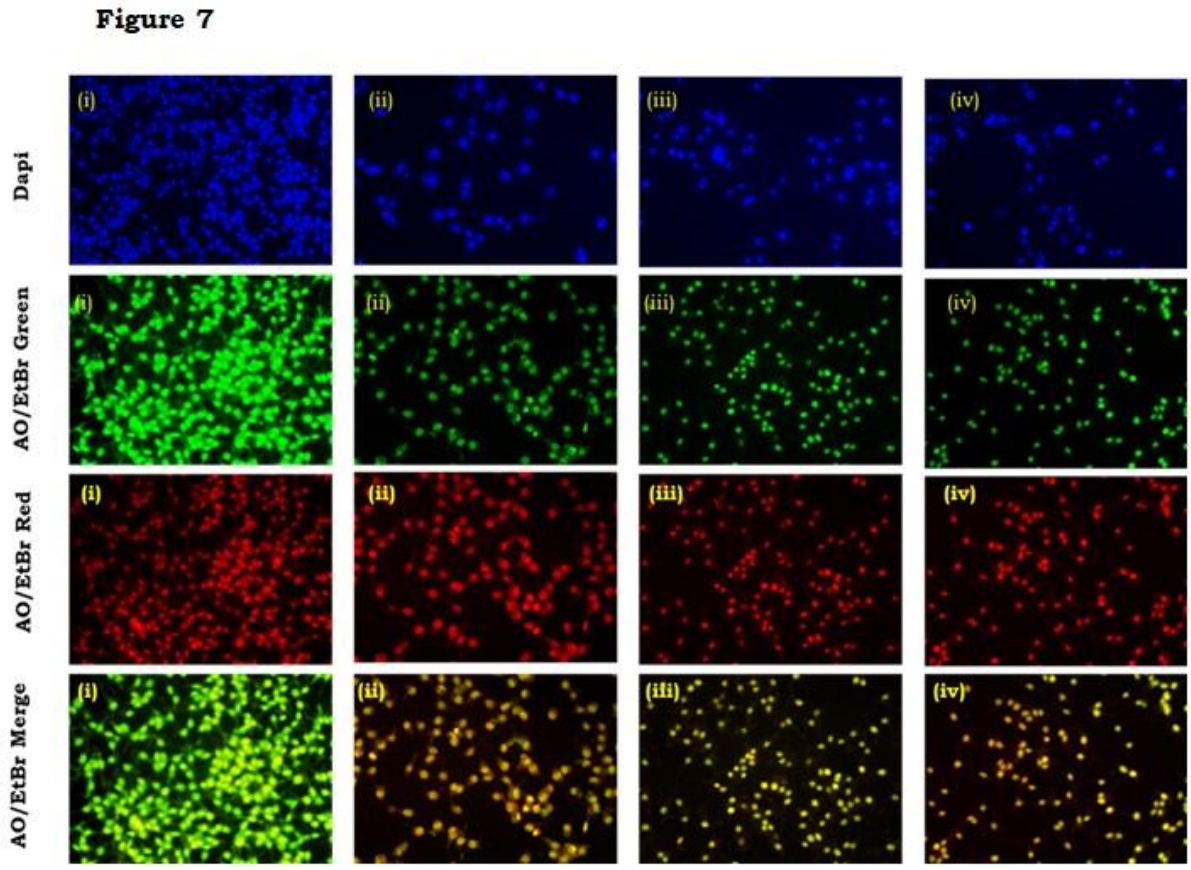

Figure 7

The diagram depicts the morphological alterations associated with apoptotic in MCF-7 cells following staining with DAPI and AO/EtBr. **(i)** Placebo Lipo **(ii)** PTX Lipo **(iii)** GLA Lipo **(iv)** PTX-GLA Lipo.

4.8.4 Detection of Apoptosis using AO/EtBr staining

A.O./EtBr staining, followed by fluorescence microscopy, revealed morphological apoptotic changes. **(Figure 7)** demonstrated that Placebo-Lipo PTX-Lipo, GLA-Lipo, and PTX-GLA-Lipo-treated MCF-7 cells showed apoptosis changes, like early apoptotic cells having yellow fluorescing nuclei, late apoptotic cells having orange to red fluorescing nuclei. Meanwhile, control MCF-7 cells show uniformly green fluorescent nuclei.

4.8.5 Mitochondrial membrane potential using JC-1 dye

The interruption of mitochondrial membrane potential ($\Delta\Psi_m$) is a key factor in early cellular apoptosis, which may be identified by observing a shift in the intensity ratio of JC-1 fluorescence from red to green. The current study found that control MCF-7 cells displayed a significantly increased ratio of red to green intensity, indicating intact mitochondrial Tran' s membrane potential. However,Placebo-Lipo PTX-Lipo, GLA-Lipo, and PTX-GLA-Lipo treatments decreased the intensity ratios from red to green, indicating a loss of mitochondrial membrane potential **(Figure 8)**.

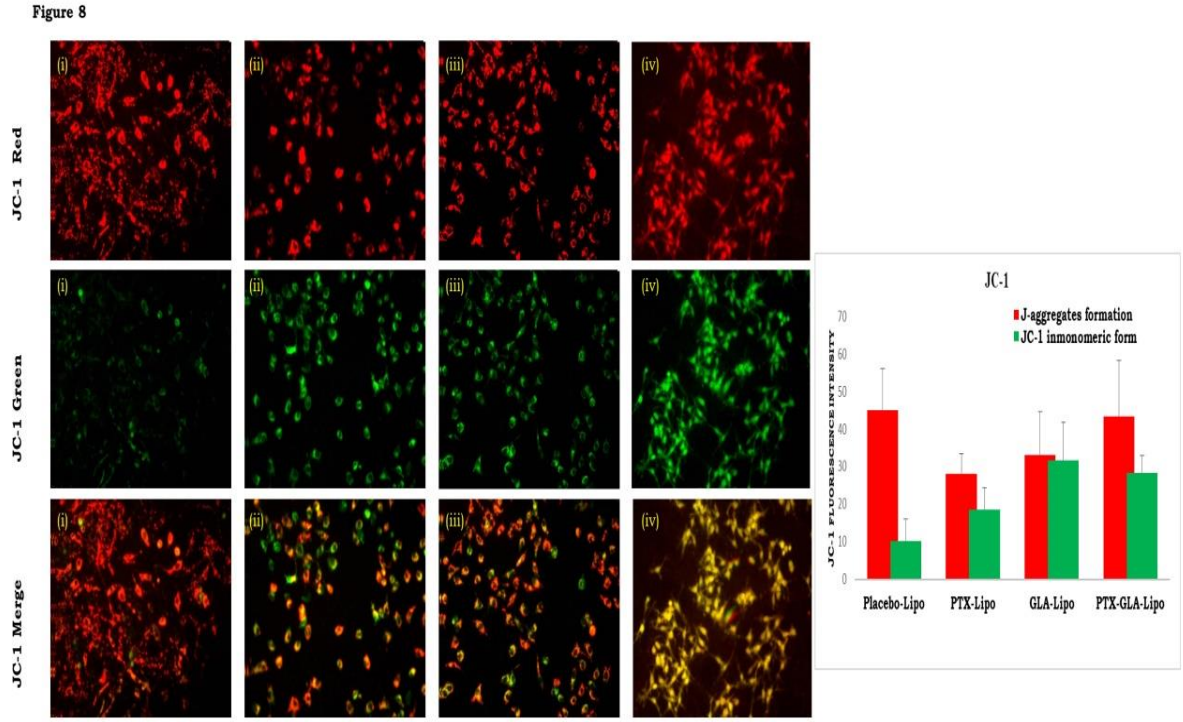

Figure 8

The MCF-7 cells were subjected to four different treatments: (i) Placebo Lipo, (ii) PTX Lipo, (iii) GLA Lipo, and (iv) PTX-GLA Lipo. The IC50 value after 24 hours. Following that, the sample was exposed to a JC-1 staining solution in order to assess alterations in mitochondrial membrane potential. These changes were observed using microscope (IX 53, Olympus, Shinjuku, Tokyo, Japan).

5. Discussion

We successfully developed PTX-loaded GLA liposomes using the thin film hydration process and optimized them using Design Expert software. The BBD design (3-level) with 3 factors and 3 responses were employed to obtain the optimized formulation. The liposomal formulations were characterized for P.S., PDI, and Z.P. to get the final optimized formulations. The values of different P.S., PDI, and Z.P. for different formulations are given in Table 1. Figure no 1 Box-Behnken experimental design illustrating the 3-D surface plots of represents the effect on P.S., PDI and Z.P [16,28]. Several parameters play a precarious role in attaining the characteristics of nanoparticles, like small size, good distribution, morphology, dispersion, and high encapsulation efficiency. These characteristics have a significant impact on the apparent direction of nanomedicine. Table 2 includes the P.S., PDI, and Z.P. values for the PTX-Liposome, GLA-Liposome, and PTX-GLA-Liposome. PTX-GLA-Liposome PS is 186.43 ± 1.03. N.P.s between 100- 200 nm are recommended size to achieve greater permeability and retention (EPR) effect in solid tumours though avoiding the trap of liver and spleen's filtering systems [29]. PDI measures particle homogeneity that varies from 0.01 (mono spread particles) to 0.5–0.7, whereas the PDI index value of >0.7 indicates the formulation's broad particle size distribution. PDI for the PTX-GLA-Liposome is approx. 0.361±0.015 is indicated the liposomes were monodisperse and homogenous [30]. FTIR is an essential method for identifying encapsulated drugs. It provides a better understanding of alterations in the quantity, nature, or frequency of chemical bonds resulting from the inclusion of PTX. The FTIR study exposed that there was no physical or chemical interaction between the excipients, drugs, and GLA. (Figure 2). The FTIR spectrum of the PTX-GLA-Lipo mixture showed very few

spectral peak shifts, which supports the idea that Paclitaxel (PTX) and (GLA) are stable and compatible. For liposomal formulations, maintaining stability is crucial to ensuring the preservation of the encapsulated drug's quality and therapeutic efficacy [31,32]. TEM and SEM analyses provided insights into the morphology of the nanoparticles. All formulations (placebo-Lipo, PTX-Lipo, GLA-Lipo, and PTX-GLA Lipo) displayed well-defined spherical shapes as observed by SEM (Figure 3A). TEM analysis (Figure 3E) further confirmed the spherical morphology of the liposomes [33,34]. Entrapment efficiency is a critical factor influencing drug efficacy and stability within liposomes. The E.E. was observed at 80.28% and 77.92% for PTX-Lipo and PTX-GLA Lipo formulations, respectively. This observation suggests a slightly greater encapsulation efficiency for PTX-Lipo, possibly due to more efficient interactions between PTX and the liposomal bilayer than the combined PTX and GLA formulation [35]. Furthermore**,** *in vitro* release of PTX from PTX-Lipo and PTX-GLA-Lipo formulations was also investigated at various time points. Both formulations exhibited sustained and continuous PTX release throughout the experiment (Figure 4). At 8 hours, PTX-Lipo and PTX-GLA-Lipo achieved release percentages of 63.88% and 59.11%, respectively. By 48 hours, these values increased to 80.34% and 77.44%, indicating the ability of both formulations to maintain therapeutic drug concentrations for extended periods. A paclitaxel standard curve was utilized to quantify release percentages, ensuring the accuracy of PTX concentration measurements at each time point [36–38]. PTX-Lipo and PTX-GLA Lipo formulations were stored at 4 ± 1°C and 40 ±2°C P.S., PDI, and Z.P. were monitored over time at these temperatures (Table 4). All formulations exhibited minimal changes in P.S., PDI, and Z.P. after 3 months, indicating excellent stability during storage. Maintaining these characteristics is crucial for the efficacy and shelf life of the

liposomal delivery system. Stability at different temperatures ensures the formulations withstand diverse storage environments [38–40]. After the characterisation of PTX-GLA liposome, an in vitro investigation was conducted to assess the cytotoxicity of the PTX-GLA liposome in MCF-7 cells using the MTT test. PTX-GLA liposomes showed significant cytotoxicity against MCF-7 cells in a way that depended on the dose. The PTX-GLA liposome exhibited a reduced IC50 value compared to the PTX liposome when tested against MCF-7 cells [41–44]. The possible reason behind this could be the combination effect and sustained release of PTX-GLA liposome. The observed differences in cellular uptake between formulations highlight the synergistic effect of PTX and GLA in promoting liposome internalization compared to the reduced uptake seen with GLA liposomes. Notably, the co-encapsulation of PTX and GLA in PTX-GLA-Lipo resulted in the highest internalization by cells, suggesting a more effective targeted delivery strategy compared to their separate use. This study demonstrates the potential of targeted liposomal drug delivery systems to enhance the effectiveness of anticancer treatments [41,45]. To confirm PTX-GLA lipo's cytotoxicity, MCF-7 cells were stained with DAPI to assess nuclear apoptosis. Lipo-treated cells showed chromatin condensation (CC) and nuclear fragmentation (N.F.), while control cells contained unaltered nuclei [46]. A.O./EtBr dual staining was used to assess PTX-GLA liposome-induced apoptosis in MCF-7 cells. Apoptotic bodies, early, and late apoptotic cells were present in PTX-GLA liposome-treated MCF-7 cells, which were green. Late apoptotic cells were orange, while early ones were bright green and yellow [47]. Considering that the depolarization of the mitochondria membrane (ΔΨm) is a crucial indicator of the initiation of cell death signalling. Additional JC-1 staining was conducted to identify the loss of mitochondrial membrane potential (ΔΨm). The mitochondrial membrane potential remains

undamaged in MCF-7 cells that have not been treated. The JC-1 dye forms J-aggregates (in its dimeric form) within the mitochondrial matrix, resulting in the emission of red fluorescence. While cells experience a reduction in mitochondrial membrane potential, JC-1 is unable to enter the mitochondrial matrix and instead remains in its individual form, resulting in the emission of green fluorescence. In this investigation, we detected the presence of green fluorescence in the groups treated with lipo, which suggests a decrease in mitochondrial membrane potential. The findings obtained from our in-vitro experiments confirm the antiapoptotic efficacy of PTX-GLA Lipo in MCF-7 cells [42,48–50].

Conclusion

This study explores the potential of GLA-based liposomes for targeted delivery of Paclitaxel (PTX) and its anticancer effects on breast cancer cells. These findings may contribute to the development of future anticancer therapies. However, PTX-GLA liposomes need further optimization for clinical application to minimize side effects and ensure proper distribution and concentration within the body. GLA, incorporated here, aims to increase the specific delivery and chemotherapeutic efficacy of PTX against MCF-7 breast cancer cells within the tumour microenvironment. As hypothesized, the PTX-GLA formulation exhibited significantly higher cellular uptake, including penetration into the nucleus and perinuclear regions. Additionally, it demonstrated improved efficacy while reducing PTX-associated toxicity. While further safety and efficacy studies are warranted, these results suggest the promising potential of PTX-GLA liposomes for future cancer treatment.

Conflict of interest

The authors reveal no conflicts of interest.

Acknowledgements

The authors express their gratitude to the Department of Pharmaceutical Sciences (DPS) at Babasaheb Bhimrao Ambedkar (A Central) University, Lucknow, for providing the necessary resources to successfully conduct the study.

References

1. Kushwah, V. *et al.* Implication of linker length on cell cytotoxicity, pharmacokinetic and toxicity profile of gemcitabine-docetaxel combinatorial dual drug conjugate. *International Journal of Pharmaceutics* **548**, 357–374 (2018).

2. Sung, H. *et al.* Global cancer statistics 2020: GLOBOCAN estimates of incidence and mortality worldwide for 36 cancers in 185 countries. *CA: a cancer journal for clinicians* **71**, 209–249 (2021).

3. Mueller, V. *et al.* Epidemiology, clinical outcomes, and unmet needs of patients with human epidermal growth factor receptor 2-positive breast cancer and brain metastases: A systematic literature review. *Cancer treatment reviews* **115**, 102527 (2023).

4. Guo, D.-D. *et al.* Synergistic anti-tumor activity of paclitaxel-incorporated conjugated linoleic acid-coupled poloxamer thermosensitive hydrogel in vitro and in vivo. *Biomaterials* **30**, 4777–4785 (2009).

5. Singla, A. K., Garg, A. & Aggarwal, D. Paclitaxel and its formulations. *International journal of pharmaceutics* **235**, 179–192 (2002).

6. Wu, C., Gao, Y., Liu, Y. & Xu, X. Pure paclitaxel nanoparticles: preparation, characterization, and antitumor effect for human liver cancer SMMC-7721 cells. *International journal of nanomedicine* 6189–6198 (2018).

7. Monteiro, N., Martins, A., Reis, R. L. & Neves, N. M. Liposomes in tissue engineering and regenerative medicine. *Journal of the Royal Society Interface* **11**, 20140459 (2014).

8. Maja, L., Željko, K. & Mateja, P. Sustainable technologies for liposome

preparation. *The Journal of Supercritical Fluids* **165**, 104984 (2020).

9. Zhang, Q. *et al.* The anticancer efficacy of paclitaxel liposomes modified with low-toxicity hydrophobic cell-penetrating peptides in breast cancer: an in vitro and in vivo evaluation. *RSC advances* **8**, 24084–24093 (2018).

10. Guimarães, D., Cavaco-Paulo, A. & Nogueira, E. Design of liposomes as drug delivery system for therapeutic applications. *International journal of pharmaceutics* **601**, 120571 (2021).

11. Nsairat, H. *et al.* Liposomes: Structure, composition, types, and clinical applications. *Heliyon* **8**, (2022).

12. Saad, S. *et al.* Novel gamma linoleic acid encased in situ lipogel for augmented anti-tumor efficacy against solid tumor: In vitro and in vivo evaluation. *Journal of Drug Delivery Science and Technology* **87**, 104768 (2023).

13. D'Angelo, S., Motti, M. L. & Meccariello, R. $ω$-3 and $ω$-6 polyunsaturated fatty acids, obesity and cancer. *Nutrients* **12**, 2751 (2020).

14. Balić, A., Vlašić, D., Žužul, K., Marinović, B. & Bukvić Mokos, Z. Omega-3 versus omega-6 polyunsaturated fatty acids in the prevention and treatment of inflammatory skin diseases. *International journal of molecular sciences* **21**, 741 (2020).

15. Roy, S., Singh, M., Rawat, A., Kumar, D. & Kaithwas, G. Mitochondrial apoptosis and curtailment of hypoxia-inducible factor-1$α$/fatty acid synthase: A dual edge perspective of gamma linolenic acid in ER+ mammary gland cancer. *Cell Biochemistry and Function* **38**, 591–603 (2020).

16. Kushwah, V., Jain, D. K., Agrawal, A. K. & Jain, S. Improved antitumor efficacy and reduced toxicity of docetaxel using anacardic acid functionalized stealth liposomes. *Colloids and Surfaces B: Biointerfaces* **172**, 213–223 (2018).

17. Want, M. Y. *et al.* Nanoliposomal artemisinin for the treatment of murine visceral leishmaniasis. *International journal of nanomedicine* 2189–2204 (2017).

18. Kumar, A. A., Harshad, H., Kaushik, T. & Sanyog, J. Improved Stability and Antidiabetic Potential of Insulin Containing Folic Acid Functionalized Polymer Stabilized Multilayered Liposomes Following Oral Administration. (2014).

19. Deepak, P. *et al.* c (RGDfK) anchored surface manipulated liposome for tumor-targeted Tyrosine Kinase Inhibitor (TKI) delivery to potentiate liver anticancer activity. *International journal of pharmaceutics* **642**, 123160 (2023).

20. Sonali *et al.* Transferrin liposomes of docetaxel for brain-targeted cancer applications: formulation and brain theranostics. *Drug delivery* **23**, 1261–1271 (2016).

21. Roy, S., Singh, M., Sammi, S. R., Pandey, R. & Kaithwas, G. ALA-mediated biphasic downregulation of $α$-7nAchR/HIF-1$α$ along with mitochondrial stress modulation strategy in mammary gland chemoprevention. *Journal of cellular physiology* **234**, 4015–4029 (2019).

22. Kim, Y. *et al.* Resveratrol inhibits cell proliferation and induces apoptosis of human breast carcinoma MCF-7 cells. *Oncology reports* **11**, 441–446 (2004).

23. Panwar, P., Pandey, B., Lakhera, P. C. & Singh, K. P. Preparation, characterization, and in vitro release study of albendazole-encapsulated nanosize liposomes. *International journal of nanomedicine* 101–108 (2010).

24. Bhalerao, S. S. & Raje Harshal, A. Preparation, optimization, characterization, and stability studies of salicylic acid liposomes. *Drug development and industrial pharmacy* **29**, 451–467 (2003).

25. Kumar, D. N. *et al.* Combination therapy comprising paclitaxel and 5-fluorouracil by using folic acid functionalized bovine milk exosomes improves the therapeutic efficacy against breast cancer. *Life* **12**, 1143 (2022).

26. Tor, Y. S. *et al.* Induction of apoptosis in MCF-7 cells via oxidative stress generation, mitochondria-dependent and caspase-independent pathway by ethyl acetate extract of Dillenia suffruticosa and its chemical profile. *PLoS One* **10**, e0127441 (2015).

27. Roy, S. *et al.* Alpha-linolenic acid stabilizes HIF-1 $α$ and downregulates FASN to promote mitochondrial apoptosis for mammary gland chemoprevention. *Oncotarget* **8**, 70049 (2017).

28. Rane, S. & Prabhakar, B. Optimization of paclitaxel containing pH-sensitive liposomes by 3 factor, 3 level box-behnken design. *Indian journal of*

pharmaceutical sciences **75**, 420 (2013).

29. Wu, J. The enhanced permeability and retention (EPR) effect: the significance of the concept and methods to enhance its application. *Journal of personalized medicine* **11**, 771 (2021).

30. Jameela Jasmine, H. Formulation and In-Vitro Evaluation of Raloxifene Hydrochloride Loaded Mixed Pluronic L121/F127 Polymeric Micelles. (College of Pharmacy, Madras Medical College, Chennai, 2017).

31. Hiremath, J. G. *et al.* Paclitaxel loaded carrier based biodegradable polymeric implants: Preparation and in vitro characterization. *Saudi Pharmaceutical Journal* **21**, 85–91 (2013).

32. Ha, P. T. *et al.* Targeted drug delivery nanosystems based on copolymer poly (lactide)-tocopheryl polyethylene glycol succinate for cancer treatment. *Advances in Natural Sciences: Nanoscience and Nanotechnology* **7**, 15001 (2016).

33. Toopkanloo, S. P. *et al.* Impact of quercetin encapsulation with added phytosterols on bilayer membrane and photothermal-alteration of novel mixed soy lecithin-based liposome. *Nanomaterials* **10**, 2432 (2020).

34. Amnuaikit, T., Limsuwan, T., Khongkow, P. & Boonme, P. Vesicular carriers containing phenylethyl resorcinol for topical delivery system; liposomes, transfersomes and invasomes. *Asian journal of pharmaceutical sciences* **13**, 472–484 (2018).

35. Han, B. *et al.* Preparation, characterization, and pharmacokinetic study of a novel long-acting targeted paclitaxel liposome with antitumor activity. *International journal of nanomedicine* 553–571 (2020).

36. Nguyen, T. L., Nguyen, T. H. & Nguyen, D. H. Development and in vitro evaluation of liposomes using soy lecithin to encapsulate paclitaxel. *International journal of biomaterials* **2017**, 8234712 (2017).

37. Nie, S., Hsiao, W. L. W., Pan, W. & Yang, Z. Thermoreversible Pluronic®F127-based hydrogel containing liposomes for the controlled delivery of paclitaxel: in vitro drug release, cell cytotoxicity, and uptake studies. *International journal of*

nanomedicine 151–166 (2011).

38. Jaradat, E., Weaver, E., Meziane, A. & Lamprou, D. A. Synthesis and Characterization of Paclitaxel-Loaded PEGylated Liposomes by the Microfluidics Method. *Molecular Pharmaceutics* **20**, 6184–6196 (2023).

39. Kan, P., Tsao, C.-W., Wang, A.-J., Su, W.-C. & Liang, H.-F. A liposomal formulation able to incorporate a high content of Paclitaxel and exert promising anticancer effect. *Journal of drug delivery* **2011**, 629234 (2011).

40. Agrawal, A. K., Urimi, D., Harde, H., Kushwah, V. & Jain, S. Folate appended chitosan nanoparticles augment the stability, bioavailability and efficacy of insulin in diabetic rats following oral administration. *RSC Advances* **5**, 105179–105193 (2015).

41. Ramasamy, T. *et al.* Polyunsaturated fatty acid-based targeted nanotherapeutics to enhance the therapeutic efficacy of docetaxel. *Drug Delivery* **24**, 1262–1272 (2017).

42. Rani, S., Ansari, M. N., Saeedan, A. S. & Kaithwas, G. Novel Quinazoline Derivative Activates FIH-1 in MCF-7 Cells and 7 , 12-Dimethylbenz [a] - Anthracene Induced Mammary Gland Carcinoma in Albino Rats. **38**, 4153–4170 (2024).

43. Xin, H. *et al.* Enhanced anti-glioblastoma efficacy by PTX-loaded PEGylated poly (ε-caprolactone) nanoparticles: in vitro and in vivo evaluation. *International journal of pharmaceutics* **402**, 238–247 (2010).

44. Gupta, U. *et al.* Enhanced apoptotic and anticancer potential of paclitaxel loaded biodegradable nanoparticles based on chitosan. *International journal of biological macromolecules* **98**, 810–819 (2017).

45. Lei, M. *et al.* Dual-functionalized liposome by co-delivery of paclitaxel with sorafenib for synergistic antitumor efficacy and reversion of multidrug resistance. *Drug delivery* **26**, 262–272 (2019).

46. Heney, M. *et al.* Effectiveness of liposomal paclitaxel against MCF-7 breast cancer cells. *Canadian journal of physiology and pharmacology* **88**, 1172–1180 (2010).

47. Banerjee, P. P. *et al.* Cytotoxic effect of graphene oxide-functionalized gold nanoparticles in human breast cancer cell lines. *The Nucleus* **62**, 243–250 (2019).

48. Sivandzade, F., Bhalerao, A. & Cucullo, L. Analysis of the mitochondrial membrane potential using the cationic JC-1 dye as a sensitive fluorescent probe. *Bio-protocol* **9**, e3128--e3128 (2019).

49. Kumar, D. *et al.* Mechanistic exploration of paclitaxel as an anticancer against the OATP3A1 transporter a computational approach. **6**, (2024).

50. Kumar, R. *et al.* Harnessing Potential of $ω$-3 Polyunsaturated Fatty Acid with Nanotechnology for Enhanced Breast Cancer Therapy: A Comprehensive Investigation into ALA-Based Liposomal PTX Delivery. *Pharmaceutics* **16**, 913 (2024).